

## ASTRONOMICAL OPTICAL INTERFEROMETRY. I. METHODS AND INSTRUMENTATION

S. Jankov

*Astronomical Observatory Belgrade, Volgina 7, 11060 Belgrade 38, Serbia*

E-mail: *sjankov@aob.rs*

(Received: November 17, 2010; Accepted: November 17, 2010)

**SUMMARY:** Previous decade has seen an achievement of large interferometric projects including 8-10m telescopes and 100m class baselines. Modern computer and control technology has enabled the interferometric combination of light from separate telescopes also in the visible and infrared regimes. Imaging with milli-arcsecond (mas) resolution and astrometry with micro-arcsecond ( $\mu$ as) precision have thus become reality. Here, I review the methods and instrumentation corresponding to the current state in the field of astronomical optical interferometry. First, this review summarizes the development from the pioneering works of Fizeau and Michelson. Next, the fundamental observables are described, followed by the discussion of the basic design principles of modern interferometers. The basic interferometric techniques such as speckle and aperture masking interferometry, aperture synthesis and nulling interferometry are discussed as well. Using the experience of past and existing facilities to illustrate important points, I consider particularly the new generation of large interferometers that has been recently commissioned (most notably, the CHARA, Keck, VLT and LBT Interferometers). Finally, I discuss the longer-term future of optical interferometry, including the possibilities of new large-scale ground-based projects and prospects for space interferometry.

**Key words.** Instrumentation: interferometers – Methods: observational – Techniques: high angular resolution

### 1. INTRODUCTION

An optical (visible and infrared) long-baseline interferometer is a device that allows astronomers to achieve a higher angular resolution than it is possible with conventional telescopes. In fact, at wavelength  $\lambda$ , the resolution of a single telescope with aperture diameter  $D$  scales as  $D/\lambda$  while the resolution of two-telescope interferometer scales as  $B/\lambda$ , where the baseline  $B$  is the distance between the telescopes. However, more severely, both are limited by the atmospheric turbulence (seeing typically  $\approx 1$  arcsecond). For this reason, a single aperture telescope

can be used as an interferometric device, but usually it is composed of an array of at least two telescopes, which sample the wavefronts of light emitted by a source at separate locations, and redirect starlight to a central location in order to recombine the sampled wavefronts and to produce interference fringes. The contrast of interference fringes, or visibility, varies according to the characteristics of the light source (for example, the size of a star or the separation between two stars in a binary system) and according to the length and orientation of the interferometer's baseline, the line connecting the two telescope apertures. It is possible to take measurements from many different baselines, most easily by waiting while the

Earth rotates. In addition, most of the new interferometers have more than two mirrors in the array and can move the apertures along tracks.

The implementation of interferometry in optical astronomy began more than a century ago with the work of Fizeau, who outlined basic concept of stellar interferometry, how interference of light can be used to measure the sizes of stars. He suggested that one could observe stars using a mask with two holes in front of a large telescope and that "it should be possible to obtain some information on the angular diameters of these stars" (Fizeau 1868). The first attempts to apply this technique were carried out soon thereafter (Stéphan 1874), although the largest reflecting telescope in existence at the time, the 80cm reflector at the Observatoire de Marseille, could not resolve any stars with a mask that had two holes separated by 65cm, and only the upper limit (0.158 arcsec) of stellar diameter could be derived. However, with a Fizeau interferometer on the 1m Yerkes refractor, Michelson (1891a,b) measured the diameters of Jupiter's Galilean satellites. Following Michelson's success Schwarzschild (1896) managed to resolve a number of double stars with grating interferometer on 25cm Munich Observatory telescope, while not long afterward, on the 2.5m telescope on Mt. Wilson, Anderson (1920) determined the angular separation of spectroscopic binary star Capella ( $\alpha$  Aur).

Although the first measurement of a stellar angular diameter was performed on the supergiant star Betelgeuse ( $\alpha$  Orionis) with Michelson's 6m stellar interferometer in 1920 (Michelson and Pease 1921), the optical interferometry was slowly evolving from a difficult laboratory experiment to a mainstream observational technique. Following the success of the 6m interferometer, Pease (with Hale) constructed a 15m interferometer but this experiment was not very successful. Due to the disappointing results from the 15m interferometer, it would be decades before significant developments inspired new activity in the optical field. The real difficulty is to combine the beams in phase with each other after they have traversed exactly the same optical path from the source through the atmosphere, each telescope, and further to the beam recombination point. This has to be done to an accuracy of a few tenths of the wavelength, which in the case of visible light, is not an obvious task, particularly because of atmospheric turbulence which makes the apparent position of a star on the sky jitter irregularly. This jitter often causes the beams in different arms of the interferometer to overlap imperfectly or not at all at any given moment. For these reasons, the optical interferometry requires extreme mechanical stability, sensitive detectors with good time resolution, and at least a simple adaptive optical system to reduce the effects of atmospheric turbulence. For these reasons, only the technologies emerging at the end of 20th century allowed the full application of optical interferometry in astronomy.

Meanwhile, advances in radar technique during World War II stimulated rapid development of radio interferometry beginning with the first radio interferometer built by Ryle and Vonberg (1946). The main reason for tremendous success concern-

ing astronomical applications is that the effects of atmospheric noise are much less pronounced at radio wavelengths. Paralelly, the development of Intensity interferometry discovered by Hanbury Brown and Twiss (1956a) inspired a new project in optical interferometry. Their basic principle describes how correlations of intensities (not electric fields) can be used to measure stellar diameters. The important point is that the technique relies on the correlation between the (relatively) low-frequency intensity fluctuations at different detectors, and that it does not rely on the relative phase of optical waves at the different detectors. The requirements for the mechanical and optical tolerances of an intensity interferometer are therefore much less stringent than in the case of "direct detection" schemes as it is Fizeau/Michelson interferometry. First results were reported soon thereafter (Hanbury Brown and Twiss 1956b), leading to the development of the Narrabri intensity interferometer. With a 188m longest baseline and blue-sensitivity, this project had a profound impact on the field of optical interferometry, measuring dozens of hot-star diameters (e.g. Hanbury Brown et al. 1967a,b, 1970, 1974a,b, Davis et al. 1970). The small bandwidths attainable with intensity interferometry limited the technique to the brightest stars, and pushed the development of so-called "direct detection" schemes, where the light is combined before detection to allow large observing bandwidths.

With the advent of lasers in visible and infrared, the benefits of radio interferometry have been pursued in optical long-baseline interferometry through heterodyne detection (e.g. Gay and Journet 1973, Assus et al. 1979). Radio interferometry functions in a fundamentally different way from optical interferometry. Radio telescope arrays are heterodyne, meaning that incoming radiation is interfered with a local oscillator signal before detection. The signal can then be amplified and correlated with signals from other telescopes to extract visibility measurements. Optical interferometers are traditionally homodyne, meaning that incoming radiation is interfered only with light from other telescope. This requires transport of the light to a central station, without the benefit of being able to amplify the signal. The other important benefit of radio interferometry is that the required accuracy for beam recombination is much more easy to achieve in radio than in optical domain. One heterodyne optical interferometer (ISI, see Section 3.1) has been built to operate at  $\approx 10\mu\text{m}$  wavelengths. As for Intensity interferometry, the technique is feasible but with small bandwidths attainable and limited to bright sources, while the homodyne optical interferometry allows large bandwidths to be used since the interfered light is detected directly. Two important steps towards modern optical interferometry have been done at the Observatoire de Calern, France:

1. Labeyrie (1970) proposed speckle interferometry, a process that deciphers the diffraction-limited Fourier spectrum and image features of stellar objects by taking a large number of very-short-exposure images of the same field. This technique can be applied to reconstruct a single image that is

free of turbulent areas, in essence an image of the object as it might appear free of atmospheric turbulence.

2. Long-baseline interferometry on a star by directly combining the electric fields before photon detection ("direct detection") was first accomplished in 1974 by Labeyrie (1975) by using a 12m baseline at the I2T interferometer.

The following section deals with the fundamental observables in astronomical optical interferometry. In Section 3. three basic designs to achieve coherent combination of light are explained in more details, while in Section 4. the basic interferometric techniques are presented. Further development in the field is described in Sections 5. and 6. while the possibilities of new ground-based and space projects are discussed in Section 7. Finally, I summarize the most important conclusions in Section 8.

## 2. INTERFEROMETRIC OBSERVABLES

### 2.1. Visibility modulus

The fringe contrast observed with an interferometer is historically called the visibility and, for the simple (two-slit) interferometer can be written as:

$$V = \frac{I_{\max} - I_{\min}}{I_{\max} + I_{\min}} = \frac{\text{Fringe amplitude}}{\text{Average intensity}} \quad (1)$$

where  $I_{\max}$  and  $I_{\min}$  denote the maximum and minimum intensity of the fringes.

Generally, the primary observable of an interferometer is the complex visibility function (the amplitude and phase), which is the Fourier transform of the object brightness distribution (van Cittert-Zernike Theorem). Let  $\tilde{I}(u, v, \lambda)$  denote the spatial Fourier transform of sky brightness  $I(s, p, \lambda)$  at the wavelength  $\lambda$ , where the Fourier frequency pair  $u, v$  (spatial frequency) is the conjugate of the spatial Cartesian coordinates  $s, p$ , respectively. Defining the complex visibility  $\tilde{V}(u, v, \lambda) = \tilde{I}(u, v, \lambda)/N$  where  $N$  is normalization factor defined so that  $|\tilde{V}(0, 0, \lambda)| = 1$ , it follows:

$$V = |\tilde{V}(u, v, \lambda)|.$$

The visibility  $V$  as defined by Eq. (1) is exactly proportional to the amplitude modulus of the image Fourier component corresponding to the spatial frequency  $(u, v) = \vec{b}/\lambda$  where  $\vec{b}$  is the baseline vector  $\vec{B}$  projected onto the plane of the sky.

The phase  $\Phi$  of the fringe pattern is equal to the Fourier phase of the same spatial frequency component but it cannot be observed since an incoming plane wave from a source is corrupted as it propagates through the turbulent atmosphere which produces atmospheric phase delays such that the phase information on the source is completely lost. Practically only the modulus of the complex visibility  $V = |\tilde{V}(u, v, \lambda)|$  (or squared visibility amplitude  $V^2$ ) is an observable quantity.

The corruption of this phase information has serious consequences, since imaging of non-centrosymmetric objects rely on the Fourier phase information encoded in this intrinsic phase of interferometer fringes. Without this information, imaging cannot be done except for simple objects such as discs or round stars. A number of strategies have been developed to circumvent these difficulties.

### 2.2. Relative phase

The technique called phase referencing relies on the fact that the relative phase can be obtained if atmospheric and instrumental noise can be controlled or compensated, for example through referencing by measuring the instantaneous phases of fringes using a reference star (Shao and Colavita 1992) or by using the same source at another wavelength. The technique, called "Differential Speckle Interferometry" (DSI) measures the relative shift of an object in different spectral bands, and its application is based on the assumption that the shift between two speckle images (instantaneous distorted images, see Section 4.1) can be related to spatial structures of the object under study. Although the phase of the spatial coherence function is corrupted by instrumental and atmospheric noise, different methods of data processing can be used to overcome this difficulty. If the two sets of speckle interferograms of the same object are recorded simultaneously at two different wavelengths, but close enough for the Point Spread Function to be the same for both channels, then their ensemble average cross-spectrum provides the information about the relative shift as a fraction of the object size. This technique was described by Beckers (1982), Jankov et al. (2001).

### 2.3. Closure phases

The closure phase measurements tell us about the symmetry of an object and is only available from a closed triangle of elements, such as three telescopes. Normally, atmospheric fluctuations disturb the fringe phase between any two interferometer elements, but these fluctuations cancel out in a closed triangle.

Considering a 3-telescope array where the phases  $\Phi_{ij}, \Phi_{jk}, \Phi_{ki}$  are intrinsic phases,  $\Phi'_{ij}, \Phi'_{jk}, \Phi'_{ki}$  are phases measured on the baselines between telescopes (i and j), (j and k), (k and i) respectively,  $\psi_i, \psi_j, \psi_k$  are the atmospheric errors introduced above telescopes (i,j,k) and  $\varepsilon_{ij}, \varepsilon_{jk}, \varepsilon_{ki}$  is the noise, it follows:

$$\Phi'_{ij} = \Phi_{ij} + \psi_i - \psi_j + \varepsilon_{ij}$$

$$\Phi'_{jk} = \Phi_{jk} + \psi_j - \psi_k + \varepsilon_{jk}$$

$$\Phi'_{ki} = \Phi_{ki} + \psi_k - \psi_i + \varepsilon_{ki}$$

Consequently the closure phase:

$$\Phi_{cl} = \Phi'_{ij} + \Phi'_{jk} + \Phi'_{ki} = \Phi_{ij} + \Phi_{jk} + \Phi_{ki} + \varepsilon_{ij} + \varepsilon_{jk} + \varepsilon_{ki}$$

is free of atmospheric phase noise (Jennison 1958).

## 2.4. Bispectrum

When analysing the speckle interferometry data, one can think of many virtual sub-apertures (with sizes equal to the coherence length  $\frac{\lambda^2}{\Delta\lambda}$ ) spread across the full telescope, with fringes forming between all the sub-aperture pairs. The speckle interferometry data can be reduced using the "bispectrum", which permits a direct inversion from the estimated Fourier amplitudes and phases. The bispectrum:

$$\tilde{B}_{ijk} = \tilde{V}_{ij} \tilde{V}_{jk} \tilde{V}_{ki}$$

is formed through triple products of the complex visibilities around a closed triangle, where  $i, j, k$  specifies the three aperture locations on the pupil of the telescope.

It was discovered that the Fourier phases could also be estimated from such data (e.g. Knox and Thompson 1974), and that the bispectrum phase is identical to the closure phase. Interestingly, the use of the bispectrum for reconstructing diffraction-limited images was developed independently (Weigelt 1977) of the closure phase techniques, and the connection between the approaches was realized only later (Roddiier 1986, Cornwell 1987).

## 3. INSTRUMENTAL DESIGNS

### 3.1. Heterodyne interferometer

The principle of a Heterodyne interferometer is to change the frequency of light at each telescope, carry to the common focus an intermediate frequency signal, and combine all these signals in order to produce fringes. Associated to each telescope is a laser, and the two beams (laser and star) are then combined with a beam splitter onto an infrared-sensitive photodiode, which produces an electric current proportional to the light intensity on it. Two light waves, those from the laser and from the star, are very close in frequency and while combining two beams, they beat together to produce a signal at lower frequency such that it becomes a radio wave.

To produce interference fringes two radio signals are overlapped instead of light beams. All of the information that is carried in the visible or infrared light wave from the star is still in the new radio signal, the only thing that is different is the wavelength. The principle of heterodyne interferometry is depicted in Fig. 1.

This method of converting the frequency of a signal from the star by mixing it with a fixed-frequency "local oscillator" is called heterodyne detection. (The term "local oscillator" refers to the laser in this case). Usually, the local oscillators are CO<sub>2</sub> lasers operating at frequencies  $\approx 10\mu\text{m}$  wavelengths. The heterodyne detection suffers from bandwidth limitations as well as additional noise contribution from laser shot-noise, which becomes progressively worse at higher frequencies. However, one of the main advantages is that the signals are converted to radio frequencies and then combined electronically using techniques from radio astronomy.

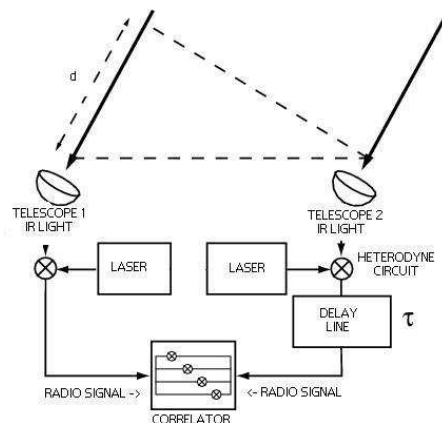


**Fig. 1.** Heterodyne interferometer arrangement. The light from an infrared laser together with infrared light from a star are converted to radio frequencies through heterodyne circuits and then combined electronically. A light wave from a star hits first telescope, and has to travel an extra distance ( $d$ ) before it arrives at second telescope. In order for the interference method to work properly, the signal from one telescope should be delayed in time ( $\tau$ ) until the wavefront reaches the other telescope; only then two signals can interfere together.

### 3.2. Intensity interferometer

The Intensity interferometer is also called "the post-detection correlation Interferometer" since the signals are correlated after detection. The intensity interferometry technique does not rely on the actual interference of light rays, thus no fringes are formed. Instead, the interferometric signal, the degree of mutual coherence, is characterized by the degree of correlation of light intensity fluctuations observed at two different detectors. In practice, the degree of mutual coherence is measured using fast temporal correlations between narrow optical waveband intensity fluctuations observed by two (or more) telescopes separated by a baseline distance (Fig. 2).

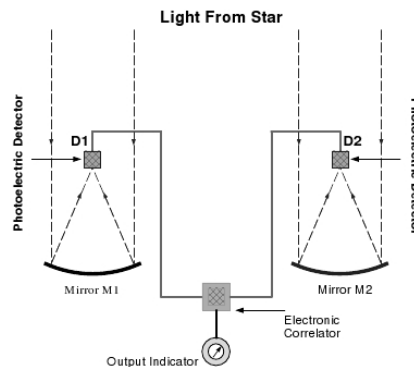


**Fig. 2.** Intensity interferometer arrangement. The interferometric signal, the degree of mutual coherence, is characterized by the degree of correlation of light intensity fluctuations observed at two different detectors.

The principal component of the intensity fluctuation is the classical shot noise which will not demonstrate any correlation between the two separated telescopes. The intensity interferometric signal is related to a smaller noise component: the wave noise. The wave noise can be understood as the "beat frequency" in optical intensity between the different Fourier components of the light reaching the telescopes. This wave noise will show correlation between the two detectors, provided there is some degree of mutual coherence between the light received at the two telescopes.

The technique has the benefit of being much less sensitive to atmospheric phase fluctuations because the signals input to the correlator have followed roughly the same path through the atmosphere. Delay tracking and local oscillator stability do not have to be very accurate. Unlike the direct (Amplitude interferometry) the Intensity interferometry is well matched to blue/visible operation, and scales to long baselines with ease (the atmospheric stability requirements are a factor of a million less stringent).

The major drawback of Intensity Interferometry is that copious quantities of light are necessary to observe the wave noise signal in the presence of the much larger shot noise. Even for brightest stars, very large light collectors ( $\approx 100\text{m}^2$  area) are necessary to have a sufficient statistical strength to observe non-Poisson fluctuations around the mean photon intensity. Mainly for this reason, the experiment conducted at Narrabri from 1963 to 1971 was the only implementation of a stellar intensity interferometer. Since then, all stellar interferometers have been based on Fizeau/Michelson's techniques.

### 3.3. Direct interferometer

In this approach the light from each aperture is carried to a common focus, combined coherently in order to detect interferometric signal (fringes). The combination of two (or more) light beams can be done in the image plane (Fizeau mode, Fig. 3a) or in the pupil plane (Michelson mode, Fig. 3b). In the Fizeau mode, the ratio of aperture diameter/separation is constant from light collection to recombination in the image-plane (homothetic pupil). In the Michelson mode, this ratio is not constant since the collimated beams have the same diameter from the output of the telescope to the recombination lens. This means the object-image relationship can no longer be described as a convolution. However, it is possible to use a relay optics after the beam-combiner so as to stack two output pupils on the top of each other with a modulation depending on the output Airy discs distance (Fig. 3c). The main advantage over the Michelson mode recombinations is conservation of the object-image convolution relation (Vakili et al. 2004).

Interferometers in which the output pupil is not a homothetic image of the input pupil, but the pattern of the subaperture centers is conserved are known as densified pupil interferometers (Labeyrie 1996). In such an arrangement, the interferometer

forms a true image of small sources at the combined focus. This is particularly attractive for arrays consisting of many telescopes, because the desired information can be obtained after deconvolution with the known point spread function.

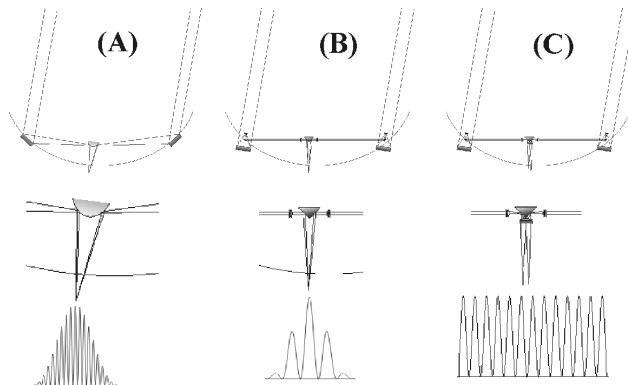


**Fig. 3.** Comparison of three different beam-combinations for an optical stellar interferometer. (A) and (B) the classical Fizeau versus Michelson beam-combinations, (C) instead of superimposing the Airy patterns from the telescopes, it is possible to use a relay lens after the beam-combiner so as to stack the two output pupils on the top of each other with a modulation depending on the output Airy discs distance.

The disadvantage of the Michelson mode is a very narrow field of view compared to the Fizeau mode, but for diluted optical arrays it is extremely difficult to construct an interferometer with image plane beam recombination. For this reason Fizeau mode is more typically implemented on a common-mount interferometers. Typical example of such an interferometer designed to create high resolution images over a wide field of view is the Large Binocular Telescope (see Section 6.7), a single-mount structure resulting in a fixed entrance pupil for which the Fizeau mode recombination is adapted.

The Michelson mode interferometry is used in long-baseline interferometers made of independent telescopes. Beam transfer optics and delay lines allow it to maintain equal path length between the telescopes as the object is tracked across the sky.

The real art of developing interferometers is to combine the beams in phase with each other after they have traversed exactly the same optical path from the source through each of the telescope down to the beam combination point. The paths are made equal by adjusting the position of mirrors in the optical delay-line (Fig. 4.) that corrects the drift induced by the diurnal rotation of the tracked star. Due to the long path lengths between the telescope and central beam combining facility, a significant differential chromatic dispersion occurs if the light is propagating in the air. In order to combine broad bandwidths, one must either transport the light through a vacuum or construct a dispersion compensator (Tango 1990).

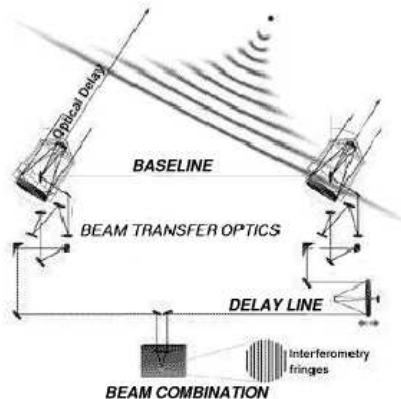


**Fig. 4.** Michelson's interferometer. The light from each aperture is carried to a common focus, combined coherently in order to detect interferometric signal (fringes). Beam transfer optics and delay lines allow it to maintain equal path length between the telescopes as the object is tracked across the sky.

In addition, mechanical constraints on the instrument, errors on the pointing model, thermal drifts, various vibrations and atmospheric turbulence make the null Optical Path Difference (OPD) point changing. The error on the OPD must be less than the coherence length defined by:  $l_c = \frac{\lambda^2}{\Delta\lambda}$  where  $\bar{\lambda}$  is the mean wavelength observed and  $\Delta\lambda$  is the spectral interval. Fringes are searched by adjusting the delay-line position, and this real-time control is called "fringetracking".

After being collected by the telescopes and properly delayed, the light must be directed to a central facility for beam combination. The interferogram can then be recorded, as long as the scanning takes place faster than the atmospheric coherence time  $\tau_c = c/\Delta\lambda$ .

## 4. INTERFEROMETRIC TECHNIQUES

### 4.1. Speckle Interferometry

Speckle interferometry is a method permitting the extraction of spatial information from two-dimensional images at scales down to the diffraction limit of the telescope, in spite of severe blurring introduced by atmospheric turbulence. The image of a star obtained through a large telescope looks "speckled" or grainy because different parts of the image are blurred by small areas of turbulence in the earth's atmosphere. The image obtained for an unresolved point source depends on the exposure time. For long exposures, the image is blurred to a seeing disk  $\approx 1$  arcsec. For exposures shorter than the coherence time ( $t_c \approx 10$ ms for the atmosphere in the optical; 100ms for the infrared), a group of bright speckles is obtained approximately of the size of the Airy disk. In that way the speckle interferometry freezes the atmosphere, and gets an instantaneously distorted image as presented in Fig. 5.

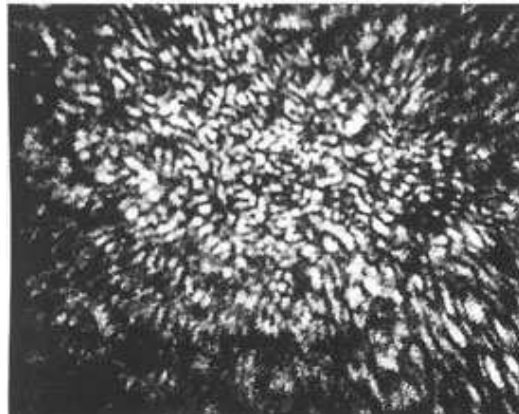


**Fig. 5.** Speckle, an instantaneously distorted stellar image.

In 1970, the French astronomer Antoine Labeyrie showed that information could be obtained on the high-resolution structure of the object from the speckle patterns using the Fourier analysis ("speckle interferometry"). In the 1980s, the methods which allowed images to be reconstructed interferometrically from these speckle patterns were developed using a sequence of short-exposure snapshots to obtain images at a telescope's diffraction limit.

With existing large telescopes, speckle techniques thus permit resolution at spatial scales of 0.025 arcseconds rather than the 1 to 2 arcseconds associated with classical techniques. These methods are also characterized by enhanced measurement accuracy of the separation of closely spaced objects seen through the turbulent atmosphere. The speckle interferometry system incorporates an intensified charge coupled device array as the primary imaging detector and an autocorrelator as a high speed data reduction processor operating at video rates. Also, the reduction of the speckle patterns can be done a posteriori involving computer processing.

### 4.2. Aperture Masking Interferometry

Aperture Masking Interferometry is a form of speckle interferometry, allowing to reach the maximum possible resolution at ground-based telescopes with large diameters to produce diffraction limited imaging.

In the aperture masking technique, the bispectral analysis (speckle masking) method is typically applied to data taken through masked apertures, where most of the aperture is blocked off and light can only pass through a series of small holes (subapertures) so that the array of holes acts as a miniature astronomical interferometer. The aperture mask removes atmospheric noise from these measurements, allowing the bispectrum to be measured more precisely than for an un-masked aperture. For simplicity the aperture masks are usually either placed in front of the secondary mirror (e.g. Tuthill et al. 2000, see Fig. 6) or placed in a re-imaged aperture plane (e.g. Young et al. 2000).

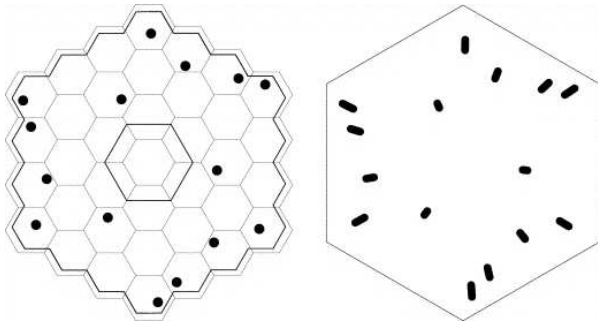


**Fig. 6.** *Desired sparse pupil (left) and the aperture mask used to generate it (right). The required pupil is shown as the set of black spots and is superimposed on a scaled version of the segmented 10m Keck primary mirror (hexagonal segments). From Tuthil et al. (2000).*

The masks are usually categorised either as non-redundant or partially redundant. Non-redundant masks consist of arrays of small holes where two pairs of holes have not the same separation vector (the same baseline). Each pair of holes provides a set of fringes at a unique spatial frequency in the image plane.

Partially redundant masks are usually designed to provide a compromise between minimising the redundancy of spacings and maximising both the throughput and the range of spatial frequencies investigated. Although the signal-to-noise of speckle masking observations at high light level can be improved with aperture masks, the faintest limiting magnitude cannot be significantly improved for photon-noise limited detectors so that the principal limitation of the technique is that it is limited to relatively bright astronomical objects.

### 4.3. Aperture Synthesis

The direct closure phase measurements together with the measurements of visibility amplitude allow one to reconstruct an image of any object using three or more independent telescopes. This technique has been successfully demonstrated by Baldwin et al. (1996) in the visible band at the Cambridge optical aperture-synthesis telescope (COAST, see Section 5.3). Each pair of telescopes in an array yields a measure of the amplitude of the spatial coherence function of the object at a spatial frequency  $\vec{b}/\lambda$  which corresponds to one point in  $(u, v)$  plane.

In order to make an image from an interferometer, one needs estimates of the complex visibilities over a large portion of the  $(u, v)$  plane, both the amplitudes and phases. The  $(u, v)$  points corresponding to a snapshot projection of the baseline are sampled from each available baseline. It is also useful to use a technique called "super-synthesis": the  $(u, v)$  plane is swept during an observation lasting several hours, due to Earth rotation. After a large variation of hour angle, several visibility moduli are, therefore, measu-

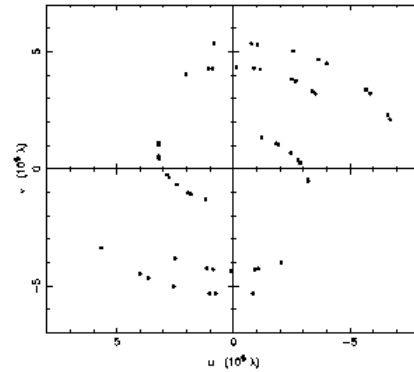


**Fig. 7.** *uv-plane coverage for the observations of Baldwin et al. (1996). Each point corresponds to an individual visibility measurement.*

red at different positions in  $(u, v)$  plane as presented in Fig. 7.

Reconstruction of complex images involves the knowledge of complex visibilities but the phase of a visibility may be deduced from closure-phase that has been applied in optical interferometry. The process after data acquisition consists of phase calibration and visibility phase reconstruction from closure-phase terms by a technique similar to bispectrum processing, so that at least three configurations of three telescope interferometer is needed. Interferometers with two apertures have limited possibilities for image reconstructions due to absence of the phase visibility recovering but in that case different spectral channels can be employed for differential visibility measurements (between the continuum and spectral line) and use of data from one part of the spectrum such as the continuum to calibrate another part (Jankov et al. 2001, 2002, 2003).

### 4.4. Nulling Interferometry

This technique, the nulling interferometry, holds a great promise for the detection and characterization of Earth-like extrasolar planets at mid-infrared wavelengths, because the light from the parent star arriving on axis is completely rejected (Bracewell 1978). The basic premise of nulling interferometry is conceptually quite simple: combine the starlight that arrives at a pair of telescopes so that at the centre of the image the two waves are exactly  $\pm\pi$  out of phase producing a dark central fringe and effectively making the central star disappear. A deep destructive fringe is to be placed across the star, but light coming from sources that are offset slightly from it (i.e. from planets) gets added rather than subtracted so that even though the star is completely blanked out, planets at the right locations (near a constructive fringe) are not attenuated (Fig. 8).

An alternative to the nulling Michelson interferometer is the use of a transparent phase-shifting mask in conjunction with a densified pupil interferometer (Boccaletti et al. 2000). The basic idea of

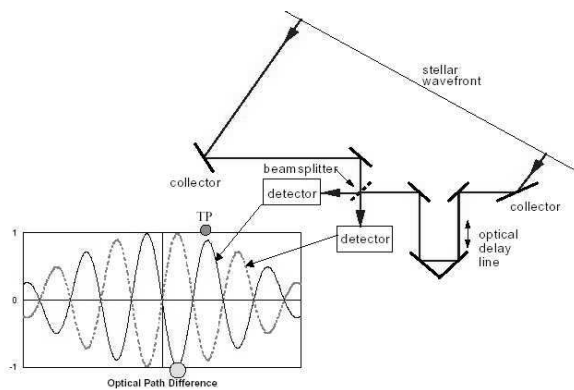


**Fig. 8.** *Nulling Interferometry Principle.* The starlight that arrives at a pair of telescopes so that a deep destructive fringe is placed across the star (making it disappear), but the light coming from a planet gets added rather than subtracted.

this concept is to introduce a  $\pm\pi$  phase shift over the central part of the point spread function produced by the densified pupil; a careful adjustment of the size of the phase mask together with pupil apodization in a coronagraphic setup can in principle provide an excellent nulling performance.

Nulling interferometry can be performed from the Earth, especially when imaging Jupiter sized planets, but the best place for viewing earth-sized planets close to their suns is from a space-based platform. Both NASA and ESA have plans to launch infrared nulling interferometry telescopes into space over the next decades (see Section 7).

## 5. PAST INTERFEROMETERS

In this section, only the most important interferometers that produced significant results in the past are presented:

### 5.1. I2T

The I2T (Interféromètre à 2 Télescopes), Observatoire Côte D’Azur, Plateau de Calern, France (Fig. 9) is the interferometer where the first direct interference fringes between separate telescopes were observed and reported by Labeyrie (1975).



**Fig. 9.** *The I2T (Interféromètre à 2 Télescopes), Plateau de Calern, France.*

I2T made observations in the visible (e.g., Blazit et al. 1977, Thom et al. 1986) and pioneered interferometry at near-IR wavelengths (di Benedetto and Conti 1983, di Benedetto 1985).

### 5.2. MARK I, II and III

The Massachusetts Institute of Technology and the Naval Research Laboratory built and operated a series of prototype interferometers, named the Mark I, Mark II, and Mark III located on Mt. Wilson, California, US.

Active fringe tracking was first demonstrated in 1979 by the Mark I interferometer (Shao and Staelin 1980), while the most popular architecture today for the moving delay line is based on the solution implemented by the Mark III interferometer (Shao et al. 1988).

The Mark III was specifically designed to perform wide-angle astrometry, but a variable baseline that could be configured from 3m to 31.5m provided the flexibility needed for a variety of astronomical programs. Because a full computer control of the siderostats and delay lines allowed automated acquisition of stars and data acquisition, it could observe up to 200 stars in a single night, until 1993, when the interferometer stopped the operation.

### 5.3. COAST

The COAST (Cambridge Optical Aperture Synthesis Telescope) operated from 1991 until 2005 at Cambridge University, England. It was planned as a coherent array of four telescopes operating in the red and near infra-red, using Michelson interferometry on baselines of up to 100m to give images with a resolution down to 1mas.

The number of telescopes (40cm apertures) has been brought up to five, and light from four of them could be interfered simultaneously. Switching between two four-telescope arrays allowed taking data on nine baselines and seven closure triangles during a single night. Observations could be carried out in the visible (R,I) or near-infrared (J,H bands). It was the first instrument of its kind to exploit the techniques of aperture synthesis and closure phase at optical or infra-red wavelengths, producing the first images from an optical aperture synthesis array (Baldwin et al. 1996).

### 5.4. IOTA

The IOTA (Infrared Optical Telescope Array) operated from 1993 to 2006 and was an interferometer of Smithsonian Astrophysical Observatory on Mt. Hopkins, Arizona, US (Fig. 10), with three 45cm telescopes (enabling closure phase observations) and baselines from 5m up to 38m. Observations have been carried out in the visible or near-IR (J,H,K bands). Visibilities with excellent calibration could be obtained with the single-mode fiber system FLUOR (Fiber Linked Unit for Optical Recombination, Coudé Du Foresto et al. 1997) which accounts for a large fraction of the astronomical results obtained with IOTA.





**Fig. 10.** *The IOTA (Infrared Optical Telescope Array) on Mt. Hopkins, US.*

### 5.5. GI2T

The GI2T (Grand Interféromètre à 2 Télescopes), Observatoire Côte D'Azur, Plateau de Calern, France (Mourard et al. 1994, see Fig. 11) was a successor of the I2T since 1985 and used two "boule" telescopes with 1.5m apertures on a north-south baseline that could be reconfigured from 10m to 65m.



**Fig. 11.** *GI2T (Grand Interféromètre à 2 Télescopes), Plateau de Calern, France.*

The GI2T had the capability of performing spectrally resolved interferometry. After closure in 2006, its beam combination table, including a versatile visible spectrograph and an IR focus has been moved to CHARA array (Mourard et al. 2009).

### 5.6. MIRA

The MIRA (Mitake Infrared Array), National Astronomical Observatory, Japan, was an ambitious plan to build a series of interferometers with increasing capabilities. The first phase of this project (MIRA-I), which consisted of two 25cm telescopes with coudé optics on a 4m baseline in Tokyo has successfully been completed in 1998, and has acquired

stellar fringes. The next step was to build an instrument with a slightly larger siderostats and a 30m baseline (MIRA-I.2). The interferometer ceased operation in 2007.

### 5.7. PTI

The PTI (Palomar Testbed Interferometer), NASA JPL, Mt Palomar, CA, US (Colavita et al. 1999, see Fig. 12) was built in 1995 and it consisted of three 40cm siderostats, up to 110m baselines which provided 3mas resolution in the near-infrared (H and K bands). It was developed primarily to demonstrate the utility of ground-based differential astrometry in the search for planets around nearby stars, and to develop key technologies for the Keck Interferometer and space-based missions.



**Fig. 12.** *PTI aerial figure. PTI is located atop Palomar Mountain, US, next to the large white dome of the historic 5m Hale Telescope.*

PTI was notable for being equipped with a "dual-star" tracking system, the first of its kind, which simultaneously tracked interference fringes from a target star and a reference star against which the target was measured. This allowed to cancel some of the atmospheric effects of astronomical seeing and to make very high precision measurements possible.

Aside from its role for the technical development of high precision "dual-star" astrometry, the PTI was used mainly for stellar diameter measurements, stellar masses and binary star work. The instrument concluded operations in 2009.

## 6. EXISTING INTERFEROMETERS

### 6.1. NPOI

The NPOI (Navy Prototype Optical Interferometer), located on Anderson Mesa near Flagstaff, Arizona, US (see Fig. 13) operates since 1995 and combines an imaging array and an astrometric facility (Armstrong et al. 1998). It can observe in

the visible with 32 spectral channels covering the wavelength range from 450nm to 850nm. The imaging subarray consists of six movable siderostats with baseline lengths from 2.0m to 437m. The array geometry has been optimized for baseline bootstrapping to facilitate the imaging of stellar surface structure. Like the Mark III, the NPOI uses vacuum delay lines for pathlength compensation. The four-element astrometric subarray of the NPOI includes an extensive site metrology system that monitors the motions of the siderostats with respect to one another in order to perform wide-angle astrometry with more than 2mas precision.



**Fig. 13.** *The NPOI (Navy Prototype Optical Interferometer), located on Anderson Mesa, US.*

### 6.2. SUSI

The SUSI (Sydney University Stellar Interferometer) is an array of 13 telescopes with 14cm apertures, operating since 1991 at Sydney University Narrabri, Australia (Davis et al. 1999, see Fig. 14). The SUSI has two beam-combining systems: The original "blue" system was designed to operate in the wavelength range 400-540 nm and employs narrow bandwidths (typically a few nanometers). The newer "red" system is designed to work in the range 500-950 nm. SUSI makes observations on a single baseline selected from a set of fixed north-south baselines with lengths ranging from 5m to 640m and it can achieve angular resolutions from 20mas to 50 $\mu$ as.

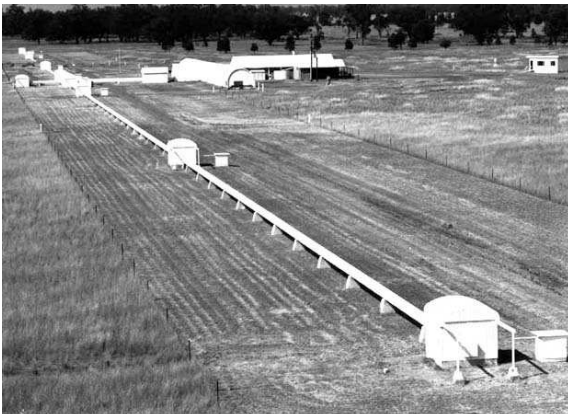


**Fig. 14.** *The SUSI (Sydney University Stellar Interferometer), Narrabri, Australia.*

The 640m baseline length, the longest of all instruments currently operational or under construction, has been chosen to resolve a sample of O stars at a wavelength of 450 nm. The focus of SUSI's observations is on improving our understanding of stellar astrophysics including: single stars (measuring effective temperatures, radii and luminosities), binary stars, (as for single stars, plus measuring distances and masses), variable stars (e.g. Cepheids and Miras), and emission line stars (e.g. Be and Wolf-Rayet stars).

### 6.3. ISI

The ISI (Infrared Spatial Interferometer), University of California at Berkeley, US is located close to the CHARA array and the former site of the Mark III on Mt. Wilson. It started operation in 1990 as two-telescope interferometer but presently consists of three 1.65m telescopes observing in the mid-infrared. The telescopes are fully mobile and their current site on Mount Wilson allows for placements as far as 70m apart providing a resolution of 3mas at 11 $\mu$ m. On July 2003, the ISI recorded its first closure phase aperture synthesis measurements.

The Fig. 15 shows three ISI's telescopes all in a line which were used for initial testing purposes, with 4m, 8m, and 12m baselines. However, they can be moved in such a way that they form a triangle and three baselines at three different angles can be measured simultaneously providing the closure phase measurements.



**Fig. 15.** *The ISI (Infrared Spatial Interferometer), Mt. Wilson, US.*

The interferometer operates at wavelengths between 9 $\mu$ m and 12 $\mu$ m and the stellar radiation is mixed with the output of a CO<sub>2</sub> laser, which acts as the local oscillator. Observations have been carried out with baseline lengths up to 56m. One of many advantages of the ISI's narrow heterodyne detection bandwidth is that one can tune the detection wavelength to be deliberately in or out of known spectral lines, allowing for interferometry on spectral lines to be carried out.

Interest of the ISI science has mainly been focused on the study of evolved stars and dust shells. However, an interferometer like the ISI is well suited

for making very precise measurements of positions of stars and particularly to measure positions of infrared stars which are hardly detectable in visible light. Investigations in the field of astrometry should help to tie the astronomical reference frames together with that established in the radio, infrared and visible.

#### 6.4. CHARA

The CHARA array, named after Center for High Angular Resolution Astronomy, Georgia State University is located on Mt Wilson, US (see Fig. 16). It consists of 6 telescopes of 1m in diameter arranged in a Y-shaped configuration with baselines ranging from 30m to 330m. First fringes on a single baseline have been obtained in November 1999 and commissioning of the full array continues. Light from the individual telescopes is conveyed through vacuum tubes to the central Beam Synthesis Facility in which the six beams can be combined together. When the paths of the individual beams are matched to an accuracy of less than one micron, after the light traverses distances of hundreds of meters, the Array then acts like a single coherent telescope for the purposes of achieving an exceptionally high angular resolution. The Array is capable of resolving details as small as  $200\mu\text{as}$ .

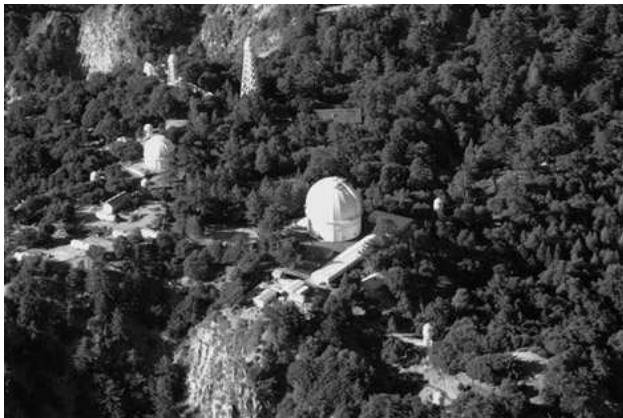


**Fig. 16.** The facilities of the CHARA (Center for High Angular Resolution Astronomy) Array together with the existing facilities of historic Mount Wilson Observatory. The Beam Synthesis Facility, an L-shaped structure of the length of a football field, can be seen close to the 2.5m telescope dome.

CHARA has entered into several collaborations with groups offering unique instruments or technologies for enhanced performance. These international collaborations have brought a significant added value to the science capabilities of the CHARA Array. At present these collaborations include a joint observing collaboration with the Observatoire de Paris through the FLUOR instrument which has been moved from the IOTA interferometer (Section 5.4) and upgraded for the CHARA Beam Synthesis Facility. A collaboration with the University of

Michigan has led to the development of an imaging beam combiner (MIRC) which has already produced the first images of stellar surfaces and close binary stars. A joint project with the University of Sydney has led to the development of a second beam combiner with significantly improved sensitivity to fainter objects while also providing measurements of very high precision. Finally, an agreement with Observatoire de la Côte d'Azur has brought the third new beam combiner (VEGA) to the Array capable of providing spectroscopic and polarimetric channels for high resolution work.

The first four-telescope fringes with VEGA Beam Combiner at the CHARA Array were obtained with CHARA (MIRC used as the infrared fringe tracker) in October 2010.

#### 6.5. KI

The KI (Keck Interferometer), NASA JPL, on Mauna Kea, Hawaii, US (Fig. 17) which consists of two 10m Keck telescopes obtained first fringes with full-apertures on March 2001.

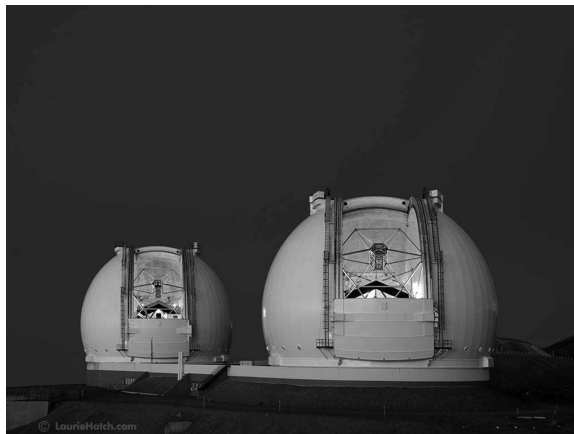


**Fig. 17.** Two 10m telescopes of the KI (Keck Interferometer) on Mauna Kea, Hawaii, US.

The 10m telescopes are equipped with high-order adaptive optics systems, which provide good correction in the near-IR and excellent wavefront quality at  $10\mu\text{m}$ . It enables the implementation of a nulling beam combiner, which will be used to characterize exo-zodiacal emission around nearby main-sequence stars. The standard science modes of the instrument are:

1.  $V^2$  mode, high sensitivity visibility amplitude measurements in the near infrared (H and K).
2. Nulling interferometry in N-band (8 -  $12\mu\text{m}$ ) to suppress light from central star and to reveal faint extended emission around it. Key scientific goals are to characterize exo-zodiacal emission around Sun-like stars to inform Terrestrial Planet Finder (see Section 7.3) mission design.
3. Differential Phase, multi-color fringe phase measurements between  $2\text{-}5\mu\text{m}$ , with direct Hot Jupiter detection (orbital parameters and masses), as the key scientific goal.

Recently, the Keck interferometer was upgraded to do self-phase-referencing (SPR) assisted K-band spectroscopy at  $R \approx 2000$ . This SPR mode as currently being implemented as the ASTrometric and phase-Referenced Astronomy (ASTRA) project will provide phase referencing and astrometric observations at the Keck Interferometer, leading to enhanced sensitivity, and the ability to monitor orbits at an accuracy level of  $30\text{-}100\mu\text{as}$ , high spectral resolution observation of Young Stellar Objects (YSO), sensitive Active Galactic Nuclei (AGN) observations, and astrometric (known exo-planetary systems characterization and galactic center general relativity) capabilities. With the first high spectral resolution mode now offered to the community, this contribution focuses on the progress of the dual field and astrometric modes.

It is planned that the KI will be upgraded with four new 1.8m "outrigger" telescopes in order to make possible imaging mode. A large fraction of the observing time available with the outriggers should be devoted to an astrometric search for extrasolar planets while the combination of all six telescopes should result in a sensitive imaging array.

## 6.6. VLTI

The VLTI (Very Large Telescope Interferometer), European Southern Observatory Paranal, Chile, obtained first fringes on the sky in March 2001, with siderostats, and presently it allows the interferometric combination of the four 8.2m telescopes (Fig. 18), augmented by four movable 1.8m auxiliary telescopes (Fig. 19).

The first generation of instruments included a commissioning instrument based on a two-telescope near-IR beam combiner VINCI (now decommissioned) as well as actually operating instruments MIDI, AMBER and PRIMA:

*MIDI* (MID-infrared Interferometric instrument) is the mid-infrared (N-band = 8 to  $13\mu\text{m}$ ) combiner which combines two beams, either from the VLT main 8.2m Unit Telescopes (UTs) or from the



**Fig. 18.** Four 8.2m main Unit Telescopes of the VLTI (Very Large Telescope Interferometer), Paranal, Chile.



**Fig. 19.** Four 1.8m Auxiliary Telescopes of the VLTI (Very Large Telescope Interferometer), Paranal, Chile.

1.8m Auxiliary Telescopes (ATs), to provide visibility moduli in the  $(u, v)$  plane. MIDI features spectroscopic optics to provide visibilities at different wavelengths within the N band and with spectral resolution  $R=30$  with the prism,  $R=230$  with the grism (a combination of a diffraction grating and prism). UT adaptive optics guarantees diffraction-limited image quality on MIDI, for targets brighter than  $V = 17^m$ . These unique capabilities allowed an access to various observing programs including observation of the Galactic Center, analysis of the nuclei of the AGN galaxies, particularly stellar and circumstellar objects, as well as solar system objects.

*AMBER* is the near-infrared instrument for the VLTI, which offers the possibility of combining two or three beams from either the UTs or the ATs. With spectral resolution up to 10 000, high visibility accuracy and the ability to obtain closure phases, AMBER offers the means to perform high quality interferometric measurements in the J,H,K bands (1- $2.5\mu\text{m}$  range). Angular resolution is set by the maximum available baseline, which is about 200 meters for the ATs and about 130 meters for the UTs. Accordingly, the limit is about 2mas for the ATs, and about 3mas for the UTs, in the K band. These design characteristics, coupled to the VLT interferometer potential, open up the access to investigations of several classes of objects, from stellar to extragalactic astronomy including, for instance, the solar system objects, low-mass stars, Cepheids, microlensing, hot exo-planets, the galactic center, nearby galaxies, and Young Stellar Objects, Luminous Blue Variables, Be stars, Novae, Wolf-Rayet and Post-AGB stars for which the results have been already published.

*PRIMA* (Phase-Referenced Imaging and Micro-arcsecond Astrometry) is a system designed to enable simultaneous interferometric observations of two objects that are separated by up to 1 arcmin, without requiring a large continuous field of view. PRIMA improves the sensitivity by using two objects (a bright star guide near a fainter target object) to bring the corrections to the atmospheric turbulences. Depending on the operation mode,

PRIMA can be used either to measure the angular separation between the two objects (astrometry mode) or to produce images of the fainter of the two objects using a phase reference technique (imaging mode). With the limiting magnitude  $K \approx 19^m$  with the UTs and  $K \approx 15^m$  with the ATs and the angular distance between the targets that can be evaluated with a resolution of  $10\mu\text{as}$ , the objects such as extra-solar planets, galactic center, Active Galactic Nuclei and extragalactic objects as well as gravitational micro-lensing are the targets for PRIMA.

In addition to these ESO's instruments there is a possibility to bring and install the visiting instruments. One of the visiting instruments *PIONIER*, developed at LAOG in Grenoble, complements existing AMBER and MIDI instruments. While AMBER has previously combined the light from three of the telescopes at the VLTI, the light coming from the four 1.8-metre Auxiliary Telescopes has been successfully combined for the first time, in October 2010. This is an important step towards unleashing the full potential of the VLTI to use multiple telescopes together.

The second generation of VLTI instruments GRAVITY, VSI and MATISSE are under development:

*GRAVITY* will coherently combine the light from all four UTs. It will provide near infrared adaptive optics assisted precision narrow-angle astrometry ( $10\mu\text{as}$ ) and interferometric phase referenced imaging ( $4\text{mas}$ ) of faint objects ( $K=20^m$ ). It will precisely measure the fringe visibility and phase of the fringe pattern to acquire spatial knowledge of the observed object. With an accuracy of  $10\mu\text{as}$ , GRAVITY will be able to study motions to within a few times the event horizon size of the Galactic Center massive black hole and potentially test the General Relativity in its strong field limit. It will be able to detect intermediate mass black holes throughout the Galaxy by their gravitational action on surrounding stars. It will directly determine masses of exo-planets and brown dwarfs, and trace the origin of protostellar jets. Also it will be capable of spatially resolving coherent gas motions in the broad line regions of Active Galactic Nuclei in external galaxies. Through its high performance infrared wavefront sensing system, GRAVITY will open up deep interferometric imaging studies of stellar and gas components in dusty, obscured regions, such as obscured active galactic nuclei, dust-embedded star forming regions, and protoplanetary disks.

*VSI* (V(LTI) Spectro-Imager) was proposed as a second-generation instrument in order to provide the community with spectrally-resolved, near-infrared images at angular resolutions down to  $1.1\text{mas}$  and spectral resolutions up to  $R = 12000$ . Targets as faint as  $K = 13^m$  will be imaged without requiring a brighter nearby reference object while fainter targets can be accessed if a suitable reference is available. The unique combination of high-dynamic-range imaging at high angular resolution and high spectral resolution enables a scientific program which serves a broad user community and at the same time provides the opportunity for breakthroughs in many areas of astrophysics. The high level specifications of the instrument are derived from

a detailed science case based on the capability to obtain milli-arcsecond resolution images of a wide range of targets including: probing the initial conditions for planet formation in the AU-scale environments of young stars; imaging convective cells and other phenomena on the surfaces of stars; mapping the chemical and physical environments of evolved stars, stellar remnants, and stellar winds, and disentangling the central regions of active galactic nuclei and supermassive black holes. The VSI will provide these new capabilities using technologies which have been extensively tested in the past. It is quite flexible instrument and should be able to make maximum use of new infrastructure as it becomes available; for example, by combining up to 8 telescopes, enabling rapid imaging through the measurement of up to 28 visibilities in every wavelength channel within a few minutes. The current studies are focused on a 4-telescope version with an upgrade to a 6-telescope one.

*MATISSE* (Multi AperTure mid-Infrared SpectroScopic Experiment) is foreseen as a mid-infrared spectro-interferometer combining up to four UTs or ATs beams. It will measure closure phase relations and thus offer an efficient capability for image reconstruction. In addition to the N band, the MATISSE will open three new observing windows at the VLTI: the L, M, and Q bands, all belonging to the mid-infrared domain. Furthermore, the instrument will offer the possibility to perform simultaneous observations in separate bands while providing several spectroscopic modes. The unique performance of the instrument is related to the existence of the four UTs that permits to push the sensitivity limits to values required by selected astrophysical programs such as the study of Active Galactic Nuclei and protoplanetary discs. Moreover, the evaluated performance of MATISSE is linked to the availability of ATs which are relocatable in position in about 30 different stations allowing the exploration of the Fourier plane with up to 200 meters baseline length. Key science programs using the ATs cover for example the formation and evolution of planetary systems, the birth of massive stars as well as the observation of the high-contrast environment of hot and evolved stars. In summary, MATISSE can be seen as a successor of MIDI by providing imaging capabilities in the entire mid-infrared accessible from the ground. The extension of MATISSE down to  $2.7\mu\text{m}$  as well as its generalization of the use of closure phases makes it also a successor of AMBER.

## 6.7. LBTI

The LBTI (Large Binocular Telescope Interferometer) on Mt. Graham, Arizona, US (Fig. 20) consists of two 8.4m telescopes mounted side by side in a single alt-azimuth mount, with a 14.4m center-to-center spacing.

This configuration offers some unique capabilities for interferometry, as it lends itself to Fizeau beam combination with a wide field of view and low thermal background. It is a fully cryogenic instrument devoted to near and mid-infrared observations ( $2\text{-}20\mu\text{m}$ ). Among the unique characteristics of the telescope are the two adaptive secondary mirrors which enable diffraction limited seeing. The system

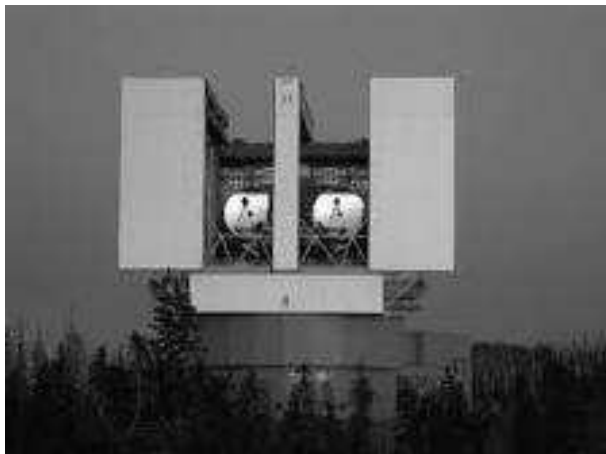


**Fig. 20.** *The LBT (Large Binocular Telescope) on Mt. Graham, US.*

is designed for high spatial resolution, high dynamic range imaging and nulling interferometry. It consists of an universal beam combiner (UBC) and three camera ports, one of which is populated currently by the Nulling and Imaging Camera (NIC).

One of the key projects for the LBTI is to survey nearby stars for debris disks down to levels which may obscure detection of Earth-like planets. A survey of approximately 80 nearby stars that is essential as a ground-based precursor of the space missions (as for example TPF/Darwin, see Sections 7.3 and 7.4). A survey will identify zodiacal disks, which signal the existence of a planetary system for follow up study with TPF/Darwin. On the other hand, the survey will also weed out those systems with very intense zodiacal emission, which can overwhelm the signal of terrestrial planets. Finally, the survey can also address the question of zodiacal emission strength as a function of spectral type and age of the central star.

In addition, the consortium of German institutes and observatories led by the Max Planck Institute for Astronomy in Heidelberg together with the Istituto Nazionale di Astrofisica in Arcetri, is developing the LINC ((L)BT (IN)terferometric (C)amera) instrument. The LINC will combine the radiation from the two 8.4m primary mirrors in Fizeau mode which allow true imagery over a wide field of view. The beam combiner will operate at wavelengths between 0.6 and  $2.4\mu\text{m}$ . When coupled with the advanced adaptive optics system of the LBT, the LINC instrument will allow the interferometric measurements over a field of approximately 10-20 arcseconds square. Ultimately, after improvement of the Adaptive Optics, which will allow better performance over a wider field of view, the instrument will be known as NIRVANA, the (N)ear-(IR) / (V)isible (A)aptive I(N)terferometer for (A)stronomy. The main scientific goals of LINC/NIRVANA are YSOs environments, circumstellar disks and outflows, formation of binary stars, stellar clusters, the compact H II regions, astrometry for extra-solar planets, the solar system minor bodies, the galactic center and the galaxies at  $z \approx 1 - 2$ .

In October 2010 the LBTI acquired its first fringes on the sky and will be interferometrically functional in 2011 once the adaptive optics and the LBTI are commissioned.

## 6.8. MROI

The MROI (Magdalena Ridge Observatory Interferometer) is presently under construction and should be operational in years to come. It is an international scientific collaboration between New Mexico Tech (US) and the University of Cambridge (UK). The Interferometer Project's mission is to develop a ten-element imaging interferometer to operate at wavelengths between  $0.6\mu\text{m}$  and  $2.4\mu\text{m}$  with baselines from 7.5m to 340m. Its primary technical and scientific goals are to produce model-independent images of faint and complex astronomical targets at resolutions over 100 times that of the Hubble Space Telescope in order to study: star and planet formation, stellar accretion and mass loss, and active galactic nuclei.

The 2.4-meter telescope achieved first light on October 2006 and commenced operations on September 2008. The work at the interferometer site started in September 2006 and the Beam Combining Facility was completed in early 2008. Presently, the telescopes are nearing their first factory acceptance tests. When finished, the interferometer will be upgraded with ten telescopes, each approximately 1.4 meters in diameter. The telescopes making up the interferometer will be spaced by distances up to 400 meters and will be optically linked in order to make aperture synthesis imaging. This setup will simulate the resolving power of a single telescope up to 400 meters in diameter. As a result of the large number of telescopes in the array, the interferometer will be able to make accurate images of complex astronomical objects.

## 7. FUTURE INTERFEROMETERS

### 7.1. OHANA

The OHANA (Optical Hawaiian Array for Nanoradian Astronomy) is the project of a hectometric fibered array at Mauna Kea, Hawaii. The concentration of large apertures on Mauna Kea (two Keck, Gemini, Subaru, CFHT, UKIRT) lends itself to ideas for interferometric combination of these six telescopes (Mariotti et al. 1996). By taking advantage of the existing adaptive optics systems, such as already installed on telescopes, this would provide excellent sensitivity and unprecedented imaging capabilities with baselines ranging from 75m to 800m (the largest baseline of OHANA (Subaru-Gemini)). This yields resolutions of 0.25mas and 0.5mas at 1 and 2 microns respectively, therefore opening the possibilities for research in many fields as for VLTI, but with four times better spatial resolution.

The OHANA project has carried out initial experiments to couple the light from Mauna Kea telescopes into a singlemode pair of 300m fibres and achieved first fringes with small prototype interfer-

ometer on July 2010, the first step in a plan to link the giant telescopes of Hawaii into a powerful optical interferometer.

## 7.2. Interferometry at Antarctica

The Dome C at Antarctica (altitude 3300m) is considered as a perfect site for astronomical interferometry due to low wind speeds, little atmospheric turbulence, negligible seismic activity and very stable climate. For this reason, several interferometric projects are under development, most notably the API (Antarctic Planet Interferometer, Swain et al. 2003) and KEOPS (Kiloparsec Explorer for Optical Planet Search, Vakili et al. 2003).

The API should be built in two phases. Phase 1 is proposed to consist of a two-element active fringe tracking interferometer using two 50cm diameter telescopes operating in a direct visibility ( $V^2$ ) mode with baselines of up to 400 metres. The H,K,L,M bands ( $1.4$  to  $5.4\mu\text{m}$ ) are to be targeted to give maximum resolution and sensitivity at up to  $10^4$  spectral resolution. In Phase 2, the full API, will consist of several 2m diameter telescopes and will be capable of operating in a variety of modes. It will be a particularly powerful tool for the study of extrasolar planets, protoplanets, Young Stellar Objects, and Active Galactic Nuclei accretion disks.

The KEOPS is proposed as three concentric rings of 1 to 2m diameter telescopes covering a diameter of 650 metres. The 36 co-phased primary telescopes would have an equivalent collecting area of at least  $60\text{m}^2$  and a resolution of a milli-arcsecond at  $10\mu\text{m}$ . KEOPS is designed for direct imaging of exo-planets in the thermal infrared, as well as for astroseismology studies.

## 7.3. TPF

The TPF (Terrestrial Planet Finder) Interferometer is a concept for a formation flying interferometer to search for Earth-like planets around nearby stars, planet studies and signs of life. TPF was being developed as a possible collaboration with ESA's Darwin mission but the project was recently cancelled.

The NASA's 2010 Decadal Survey recommended a continuation of technology development for nulling interferometry under the title of "New Worlds Technology Development Program" and now, although TPF no longer exists as a planned mission within NASA, some technology work continues. Efforts in 2009 and 2010 have included broadband nulling with the Adaptive Nuller and demonstrations with the Planet Detection Testbed. One of the possible configurations of a space interferometer (an option considered for Terrestrial Planet Finder) is presented in Fig. 21.

At present, NASA continues to work with University scientists and industry to develop the TPF technology. Meanwhile, the Kepler mission will collect information on the number of possible nearby Earthlike planets, while the Keck Interferometer and Large Binocular Telescope Interferometer projects will measure, for this purpose, the dust surrounding those stars.

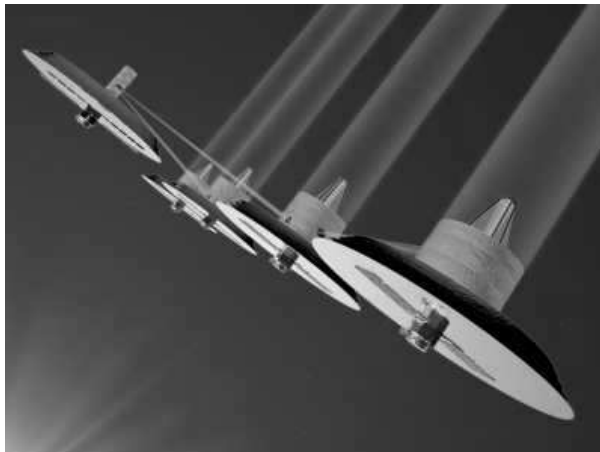


**Fig. 21.** A possible configuration of a space interferometer.

## 7.4. Darwin

The Darwin mission was planned as a constellation of four or five spacecrafts, with primary goal to look for Earth-like planets and analyse their atmospheres for chemical signatures of life. One spacecraft would have acted as a central communications station. The other three/four would have functioned as light collectors, redirecting light beams to the central station. The constellation was also intended to carry out high-resolution imaging using aperture synthesis, to provide images of celestial objects with unprecedented detail. Instead of orbiting Earth, Darwin was proposed to be placed beyond the Moon. At a distance of 1.5 million km from Earth, in a direction opposite to that of the Sun, Darwin would have operated from the second Lagrange point L2. The Darwin mission was proposed in 2007 as a concept for Phase A Study within ESA's Cosmic Vision, which includes missions beyond 2015. It was not chosen for further study, but a similar project should be re-proposed to ESA. Whatever the final design of the telescopes, it is clear that the TPF/Darwin technology will be a pathfinder for future micro and nano-arcsecond resolution instruments at infrared and other wavelengths.

## 8. CONCLUSION

After decades of development, optical interferometry is now beginning to play a major role in astrophysics. The emergence of large interferometers, in particular the Very Large Telescope interferometer, CHARA, the Keck Interferometer and Large Binocular Telescope Interferometer promise to revolutionize the impact of high resolution observations in many areas of astrophysics. Current programs execute increasingly varied and sophisticated observations. Initially, these were almost exclusively observations of stars and circumstellar phenomena, but recently, optical interferometry extended even to extragalactic targets.

The field is currently driven forward by the activities in many research areas, and important scientific results are expected in the near future. Clearly, the main beneficiaries will be stellar astrophysics and

galactic astronomy, in particular the areas of fundamental stellar properties, star and planet formation, and all stages of stellar evolution, but increasingly, optical interferometry will play more important role in other areas of astrophysics particularly exo-planetary and extragalactic research.

*Acknowledgements* – This work has been supported by the Ministry of Science and Technological Development of the Republic of Serbia (Project No 146007 "Inverse problems in astrophysics : Interferometry and Spectrophotometry of stars").

## REFERENCES

- Anderson, J. A.: 1920, *Astrophys. J.*, **51**, 263.  
 Armstrong, J. T., Mozurkewich, D., Rickard, L. J., Hutter, D. J., Benson, J. A. et al.: 1998, *Astrophys. J.*, **496**, 550.  
 Assus, P., Choplin, H., Cortegiani, J. P., Cuot, E., Gay, J., Journet, A., Merlin, G. and Rabbia, Y.: 1979, *J. Opt.*, **10**, 345.  
 Baldwin, J. E., Beckett, M. G., Boysen, R. C. et al.: 1996, *Astron. Astrophys.*, **306**, L13.  
 Beckers, J. M.: 1982, *Optica Acta*, **29**, 361.  
 Blazit, A., Bonneau, D., Josse, M., Koechlin, L., Labeyrie, A. and Oneto, J. L.: 1977, *Astrophys. J.*, **217**, L55.  
 Boccaletti, A., Riand, P., Moutou, C., Labeyrie, A.: 2000, *Icarus*, **145**, 628.  
 Bracewell, R. N.: 1978, *Nature*, **274**, 780.  
 Colavita, M. M., Wallace, J. K., Hines, B. E., Gursel, Y., Malbet, F. et al.: 1999, *Astrophys. J.*, **510**, 505.  
 Cornwell, T. J.: 1987, *Astron. Astrophys.*, **180**, 269.  
 Coudé Du Foresto, V., Ridgway, S., Mariotti, J. M.: 1997, *Astron. Astrophys. Suppl. Series*, **121**, 379.  
 Davis, J., Morton, D. C., Allen, L. R. and Hanbury Brown, R.: 1970, *Mon. Not. R. Astron. Soc.*, **150**, 45.  
 Davis, J., Tango, W. J., Booth, A. J., Brummelaar, T. A., Minard, R. A., Owens, S. M.: 1999, *Mon. Not. R. Astron. Soc.*, **303**, 773.  
 Di Benedetto, G. P., Conti, G.: 1983, *Astrophys. J.*, **268**, 309.  
 Di Benedetto, G. P.: 1985, *Astron. Astrophys.*, **148**, 169.  
 Di Benedetto, G. P., Rabbia, Y.: 1987, *Astron. Astrophys.*, **188**, 114.  
 Fizeau, H.: 1868, *C. R. Acad. Sci.*, **66**, 932.  
 Gay, J., Journet, A.: 1973, *Nature Phys. Sci.*, **241**, 32.  
 Hanbury Brown, R., Twiss, R.: 1956a, *Nature*, **177**, 27.  
 Hanbury Brown, R., Twiss, R.: 1956b, *Nature*, **178**, 1046.  
 Hanbury Brown, R., Davis, J., Allen, L. R.: 1967a, *Mon. Not. R. Astron. Soc.*, **137**, 375.  
 Hanbury Brown, R., Davis, J., Allen, L. R., Rome, J. M.: 1967b, *Mon. Not. R. Astron. Soc.*, **137**, 393.  
 Hanbury Brown, R., Davis, J., Herbison-Evans, D., Allen, L. R.: 1970, *Mon. Not. R. Astron. Soc.*, **148**, 103.  
 Hanbury Brown, R., Davis, J., Allen, L. R.: 1974a, *Mon. Not. R. Astron. Soc.*, **167**, 121.  
 Hanbury Brown, R., Davis, J., Lake, R. J. W., Thompson, R. J.: 1974b, *Mon. Not. R. Astron. Soc.*, **167**, 475.  
 Jankov, S., Vakili, F., Dominiciano de Souza, Jr., Janot-Pacheco, E.: 2001, *Astron. Astrophys.*, **377**, 721.  
 Jankov, S., Vakili, F., Domiciano de Souza Jr., A., Janot-Pacheco, E.: 2002, *ASP Conf. Series*, eds. C. Aerts, T. R. Bedding and J. Christensen-Dalsgaard, **259**, 172.  
 Jankov, S., Vakili, F., Domiciano de Souza, A.: 2003 *IAU Symp.*, **210**, 16.  
 Jennison, R. C.: 1958, *Mon. Not. R. Astron. Soc.*, **118**, 276.  
 Knox, K. T., Thompson, B. J.: 1974, *Astrophys. J.*, **193**, L45.  
 Labeyrie, A.: 1970, *Astron. Astrophys.*, **6**, 85.  
 Labeyrie, A.: 1975, *Astrophys. J.*, **196**, L71.  
 Labeyrie, A.: 1996, *Astron. Astrophys. Suppl. Series*, **118**, 517.  
 Mariotti, J. M., Coudé du Foresto, V., Perrin, G., Zhao, P., Léna, P.: 1996, *Astron. Astrophys. Suppl. Series*, **116**, 381.  
 Michelson, A. A.: 1891a, *Publ. Astron. Soc. Pacific*, **3**, 274.  
 Michelson, A. A.: 1891b, *Nature*, **45**, 160.  
 Michelson, A. A.; Pease, F. G.: 1921, *Astrophys. J.*, **53**, 249.  
 Mourard, D., Tallon-Bosc, I., Blazit, A., Bonneau, D., Merlin, G. et al.: 1994, *Astron. Astrophys.*, **283**, 705.  
 Mourard, D., Clausse, J. M., Marcotto, A., Perraut, K., Tallon-Bosc, I., Brio, Ph., Blazit, A., Bonneau, D., Bosio, S., Bresson, Y. et al.: 2009, *Astron. Astrophys.*, **508**, 1073.  
 Petrov, R. G.: 1988, *Diffraction-Limited Imaging with Very Large Telescopes*, eds. D. M. Al-loin, J. M. Mariotti (Kluwer), 249.  
 Roddier, F.: 1986, *Opt. Commun.*, **60**, 145.  
 Ryle, M., Vonberg, D. D.: 1946, *Nature*, **158**, 339.  
 Schwarzschild, K.: 1896, *Astron. Nachr.*, **139**, 353.  
 Shao, M., Staelin, D. H.: 1980, *Appl. Opt.*, **19**, 1519.  
 Shao, M., Colavita, M. M., Hines, B. E., Staelin, D. H., Hutter, D. J.: 1988, *Astron. Astrophys.*, **193**, 357.  
 Shao, M., Colavita, M. M.: 1992, *Astron. Astrophys.*, **262**, 353.  
 Stéphan, E.: 1874, *C. R. Acad. Sci.*, **78**, 1008.  
 Swain, M. R., Coudé du Foresto, V., Fossat, E., Vakili, F.: 2003, *Mem. Soc. Astron. It. Suppl.*, **2**, 207.  
 Tango, W. J.: 1990, *Appl. Opt.*, **29**, 516.  
 Thom, C., Granes, P., Vakili, F.: 1986, *Astron. Astrophys.*, **165**, L13.  
 Tuthill, P. G., Monnier, J. D., Danchi, W. C., Wishnow, E. H., Haniff, C. A.: 2000, *Publ. Astron. Soc. Pacific*, **112**, 555.  
 Vakili, F., Aristidi, E., Fossat, E., Abe, L., Domiciano, A., Belu, A., Agabi, A., Schmider, F. X., Lopez, B., Swain, M.: 2003, SF2A-2003: Semaine de l'Astrophysique Française, eds. F. Combes, D. Barret and T. Contini, EdP-Sciences, 365.  
 Vakili, F., Aristidi, E., Abe, L., Lopez, B.: 2004, *Astron. Astrophys.*, **421**, 147.  
 Weigelt, G. P.: 1977, *Opt. Commun.*, **21**, 55.  
 Young, J. S. et al.: 2000, *Mon. Not. R. Astron. Soc.*, **315**, 635.



**АСТРОНОМСКА ОПТИЧКА ИНТЕРФЕРОМЕТРИЈА.  
I МЕТОДЕ И ИНСТРУМЕНТИ****S. Jankov***Astronomical Observatory Belgrade, Volgina 7, 11060 Belgrade 38, Serbia*E-mail: *sjankov@aob.rs*

УДК 520.36-13

*Прегледни рад по позиву*

Претходна декада је видела остварење великих интерферометријских пројеката укључујући телескопе класе 8-10м и стометарске интерферометријске базе. Модерни компјутери и контролна технологија су омогућили интерферометријску комбинацију светлости са раздвојених телескопа како у видљивом тако и у инфрацрвеном режиму. Осликавање са резолуцијом од милилучне секунде и астрометрија са прецизношћу од микро-лучне секунде су тако постале реалност. Овде дајем преглед метода и инструментације које одговарају текућем стању у области астрономске оптичке интерферометрије. Прво, овај преглед сумаризује развој од пионирских радова Физоа и Мајкелсона. Затим су описане основне доступне величине а

ципима конструкције модерних интерферометара. Основне интерферометријске технике као што су интерферометрија "спекл" и "апертурних маски", "синтеза апертуре" и "нулинг" интерферометрија су такође дискутовани. Користећи искуство стечено од прошлих и постојећих инструмената да бих илустровао важне ставке, посебно разматрам нову генерацију великих интерферометара који су недавно стављени у употребу (посебно ЧАРА, КЕК, ВЛТ и ЛБТ интерферометри). На крају дискутујем дугорочну будућност оптичке интерферометрије укључујући могућност нових великих пројеката за земаљске опсерваторије као и предвиђања за космичку интерферометрију.